

Miniaturized Dual-Mode Dual-Band BPF Using a Single Square Patch Loaded Stepped-Impedance Square Open Loop Resonator

Jin Xu

School of Electronics and Information
Northwestern Polytechnical University, Xi'an, 710072, P.R. China
xujin227@nwpu.edu.cn

Abstract — This letter presents a dual-mode dual-band Bandpass Filter (BPF) using a single Square Patch Loaded Stepped-Impedance Square Open Loop Resonator (SPLSISOLR). The first four Transmission Poles (TPs) of SPLSISOLR can be tuned freely. A pair of high-impedance microstrip lines coupled with the resonator are employed to excite these four TPs to build up a dual-mode dual-band BPF, with two TPs in each passbands. The tapped point of the $50\ \Omega$ feeding lines can be freely sliding on the high impedance microstrip lines, which increases the design freedom of external quality factor of two passbands. To validate the proposed method, a dual-band filter centered at 1.79/5.42 GHz with -3 dB fractional bandwidth of 4.5%/22.5% and compact size of $0.15\lambda_g \times 0.14\lambda_g$ are designed. The fabricated filter has the merits of high band-to-band isolation, wide stopband, DC block and simple design procedure.

Index Terms — Bandpass Filter (BPF), dual-band, dual-mode, open loop resonator, patch resonator.

I. INTRODUCTION

With the development of modern dual-band wireless systems, dual-band Bandpass Filter (BPF) is great in demand for a single RF module to handle dual communication modes. So far, several dual-band BPFs have been studied in the past few years [1-3]. However, at least two resonators are used in the dual-band BPFs reported in [1-3], which may result in a relatively large circuit area. Dual-mode dual-band BPF using a single resonator becomes a good candidate and has been widely, owing to its compact size, high performance, simple physical configuration and design procedure [4]-[9].

Most of the reported dual-mode dual-band BPFs with a single resonator are realized by a ring resonator [4]-[6] or patch resonator [7]-[9]. By introducing the perturbations, such as C-sections in [4], loaded open stubs in [5], capacitive coupling in [6], embedded pair of slots in [7], cross slot and two sets of loaded stub in [8], arc- and radial-oriented slots in [9], many more modes are excited or are capable of being tuned to form the dual-mode second passband. These reported filters exhibit their own merits, but it has to admit that they also suffer from many drawbacks. The dual-band filters reported in [4], [5], [8], [9] have a less than 15 dB band-to-band isolation and suffer from a notch-like stopband on the upper stopband of the second passbands. Moreover, the dual-band filters reported in [8] and [9] lack of DC block function. In addition, two dual-mode dual-band structures presented in [6] and [7] have a lower central frequency ratio of two passbands.

In [10], a circular patch loaded uniform-impedance circular open loop resonator is proposed to exploit a dual-mode single band BPF. By using source-load coupling, transmission zeros are introduced and located on both sides of the passband, leading to a high passband skirt. In this paper, a novel Square Patch Loaded Stepped-Impedance Square Open Loop Resonator (SPLSISOLR) is proposed to exploit a dual-mode dual-band BPF. The first four Transmission Poles (TPs) are utilized and fed by a pair of high-impedance microstrip lines capacitively coupled with the resonator. The $50\ \Omega$ feeding lines are directly connected to the high-impedance microstrip lines, and the tapped point of the $50\ \Omega$ feeding lines can be freely sliding on the high-impedance microstrip lines to increase the design

freedom of external quality factor of two passbands. As an example, a dual-mode dual-band BPF centered at 1.79/5.42 GHz with -3 dB fractional bandwidth of 4.5%/22.5% is designed. The designed filter exhibits compact size, good return loss, high passband skirt and simple design procedure. Good agreement can be observed between the simulation and the measurement.

II. ANALYSIS OF SPLSISOLR

Figure 1 depicts the physical configuration of proposed SPLSISOLR, which mainly consists of three sections: i.e., a Square Patch Resonator (SPR), a stepped-impedance square Open Loop Resonator (OLR), and a pair of High-Impedance Microstrip Lines (HIML) capacitively coupled with the resonator. The space between the SPR and the stepped-impedance square OLR is equidistant and equals to S_1 . Compared with the dual-mode single-band filter presented in [10], the appearance of the resonator is changed from circular shape to square shape, which is benefit for building up the second passband. The uniform-impedance OLR is changed to be a stepped-impedance one for the sake of providing many more design freedoms. The SPLSISOLR proposed here is designed on the substrate Arlon DiClad 880 ($h=0.508$ mm, $\epsilon_{re}=2.2$, $\tan\delta=0.0009$). The width of 50Ω feeding line W_f is chosen to be 1.55 mm. As stated in [7]-[10], a larger L_{sp} can lead to lower TPs. Additionally, L_{sp} mainly affects even-mode resonant poles, but has almost no effect on odd-mode resonant poles [10]. To analyze the property of proposed SPLSISOLR simply, L_{sp} is set to be 15 mm in the following discussion. Under the physical dimensions selected as $W_1=W_2=0.8$ mm, $S_1=1$ mm, $S_2=5$ mm, $W_c=0.2$ mm, $S_c=0.5$ mm, $d_t=1.8$ mm and $L_c=7$ mm, Fig. 2 plots a typical weakly coupling frequency response of proposed SPLSISOLR. As shown, the first four TPs ($f_{p1}-f_{p4}$) are into two groups, with two TPs in each group. If appropriate coupling coefficient and external quality factor are applied to the SPLSISOLR, a dual-mode dual-band can be designed. f_{p1} close to f_{p2} can form the first passband, while f_{p3} together with f_{p4} is able to build up the second passband. As seen in Fig. 2, the bandwidth of the first passband (BW1) will be much smaller than the bandwidth of second passband (BW2). The fifth TP f_{p5} is close to the second passband, which will result in a

spurious passband if physical dimensions are not carefully selected.

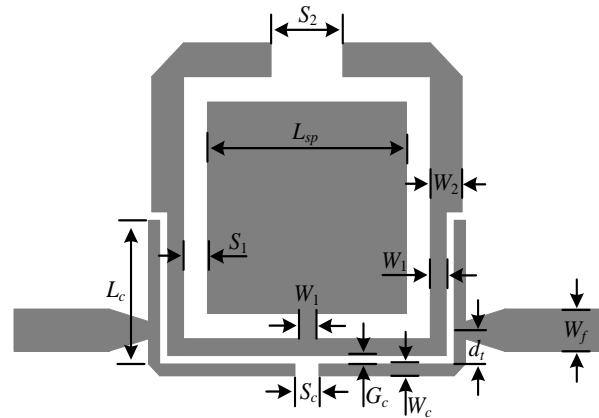


Fig. 1. Physical configuration of proposed SPLSISOLR.

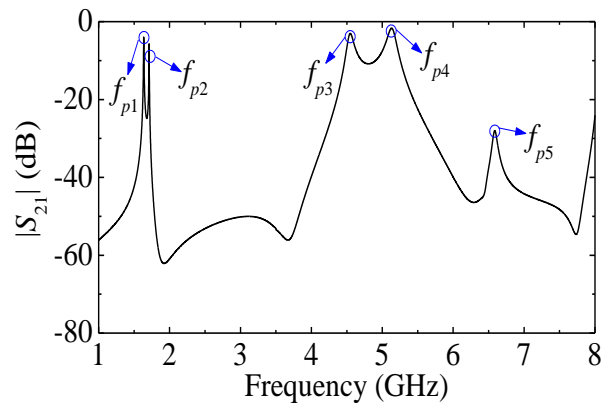


Fig. 2. Typical weakly coupling frequency response of SPLSISOLR under $G_c=0.5$ mm.

There are various physical dimensions which can be tuned to achieve the desired filter performance. The coupling coefficient of the designed filter can be tuned by L_c and G_c . The gap G_c is usually very narrow to provide a strong coupling. Figure 3 plots the simulated $|S_{21}|$ versus varied L_c . A longer L_c can increase the coupling degree, but too long L_c will bring spurious passband close to the second passband. So that the length of L_c should be selected neither too short to achieve enough coupling degree, nor too long to suppress the spurious frequency response. Figures 4, 5 and 6 plot the simulated $|S_{21}|$ versus varied W_1 , S_2 and W_2 , respectively. As W_1 increases, BW1

increases while the second passband shift towards lower frequency apparently. As S_2 increases, both the first passband and the second passband move towards higher frequency. Meanwhile, BW1 becomes narrower. W_2 has almost no effect on the performance of the second passband, but BW1 becomes wide and the first passband moves towards lower frequency as W_2 increases. It is noted that BW2 does not change dramatically as W_1 , S_2 and W_2 varies. In addition, although the variation of W_1 , S_2 and W_2 will affect the spurious passband, this can be then tuned by the length of L_c . Therefore, the frequency position and the bandwidth of two passband can be easily tuned by these physical dimensions.

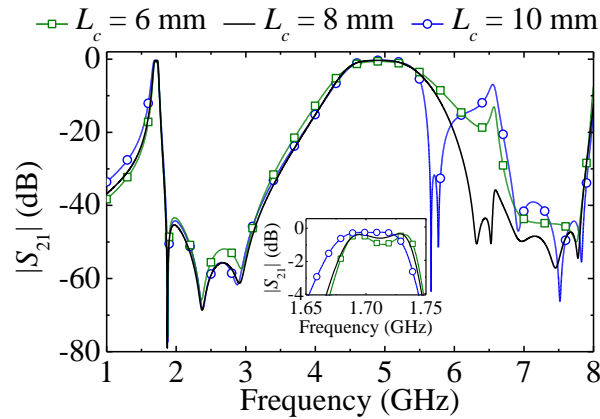


Fig. 3. Simulated $|S_{21}|$ versus varied L_c under $G_c=0.1$ mm.

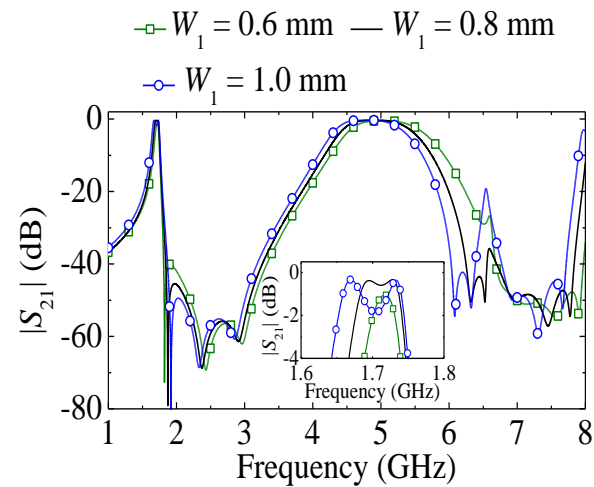


Fig. 4. Simulated $|S_{21}|$ versus varied W_1 under $G_c=0.1$ mm.

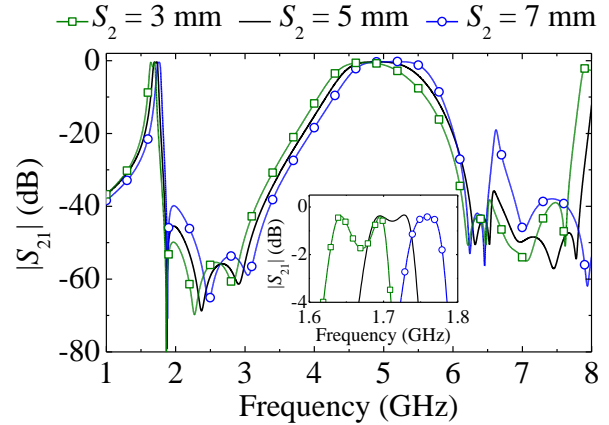


Fig. 5. Simulated $|S_{21}|$ versus varied S_2 under $G_c=0.1$ mm.

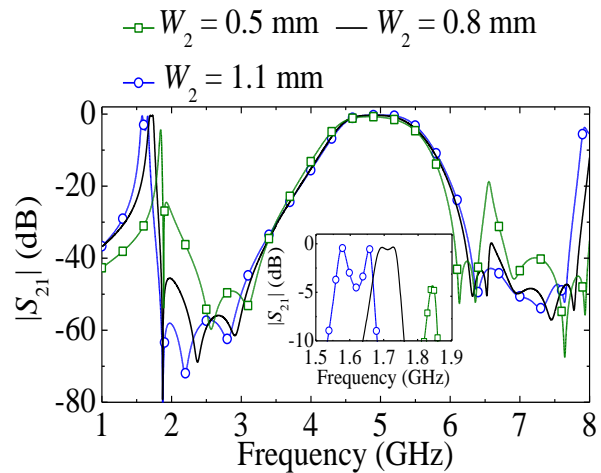


Fig. 6. Simulated $|S_{21}|$ versus varied S_2 under $G_c=0.1$ mm.

III. DUAL-MODE DUAL-BAND BPF DESIGN

To verify the proposed method, a dual-mode dual-band BPF shown in Fig. 1 is designed on the substrate Arlon DiClad 880 ($h=0.508$ mm, $\epsilon_{re}=2.2$, $\tan\delta=0.0009$). The SPLSISOLR is optimized in 3-D full wave EM simulator HFSS. After W_1 and S_2 are tuned to achieve the desired frequency position and bandwidth of two passbands, W_2 can then be tuned to separate the performance of the first passband. L_c is optimized to achieve the desired coupling coefficient and also suppress the spurious passband. The tuned physical dimensions of SPLSISOLR are $L_{sp}=14.2$ mm, $W_1=0.62$ mm, $L_{11}=7.79$ mm, $L_{12}=7.5$ mm, $S_1=1.0$ mm, $W_2=0.73$

mm, $L_{21}=8.7$ mm, $L_{22}=4.975$ mm, $W_c=0.2$ mm, $G_c=0.09$ mm, $L_{c1}=8.12$ mm, $L_{c2}=8.56$ mm and $S_c=0.5$ mm. Figure 7 plots the external quality factor of two passbands against d_t . As d_t increases, the external quality factor of the first passband (Q_{e1}) decreases, while the external quality factor of the second passband (Q_{e2}) keeps almost constant at about the value of 5. Thus, BW1 can be easily controlled by d_t . In our design, $d_t=1.8$ mm is selected to provide the appropriate external quality factor for two passbands.

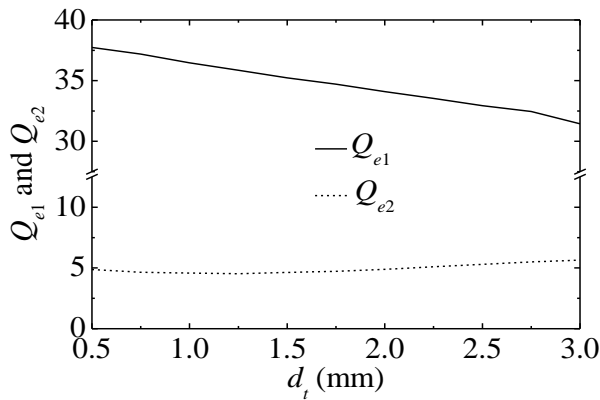


Fig. 7. Variation of Q_{e1} and Q_{e2} against varied d_t .

The overall circuit size excluding 50 Ω feeding lines is 18.02 mm \times 17.84 mm, corresponding to $0.15\lambda_g \times 0.14\lambda_g$, where λ_g represents the guided wave-length of 50 Ω microstrip line at the central frequency of the first passband. Figure 8 shows the photograph of fabricated filter. Figure 9 plots the simulated and measured S -parameters of the fabricated filter. Good agreement can be observed between the simulation and measurement. There are some discrepancies which are attributed to the fabrication error as well as SMA connectors. The measured central frequencies and -3 dB FBW of two passbands are 1.79/5.42 GHz and 4.5%/22.5%, respectively. The measured Insertion Loss (IL) at two central frequencies are 2.8/1.1 dB, while the return losses of two passbands are better than 20 dB. The band-to-band isolation is better than 30 dB from 1.91 GHz to 3.52 GHz. The fabricated filter also has -20 dB rejection level stopband from 6.45 GHz to 8.59 GHz.

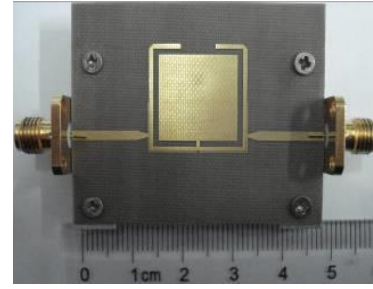


Fig. 8. Photograph of the fabricated filter.

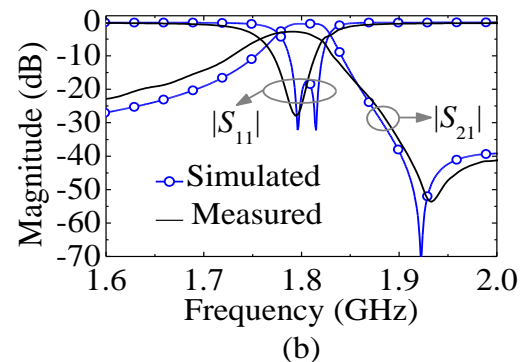
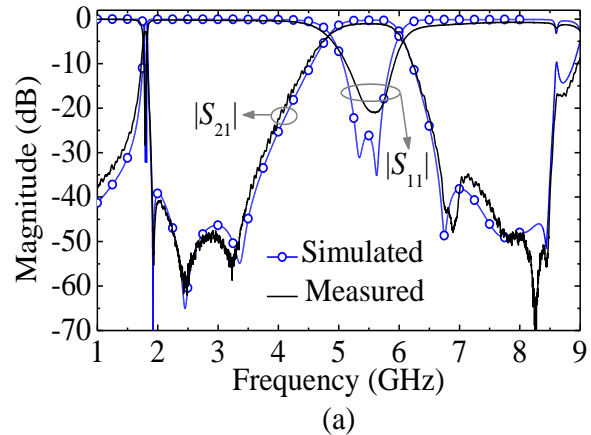


Fig. 9. Simulated and measured results of the fabricated filter: (a) wideband view, and (b) narrow-band view of the first passband.

Table 1 gives a performance comparison of this work with the reported dual-mode dual-band BPFs using a single resonator. After comparison, it can be easily found that it exhibits the merits of higher isolation and more compact sizes. Moreover, the designed filter has a larger dual-band central frequency ratio. In addition, this work

also exhibits the best out-of-band rejection performance compared with the reported works in [4]-[9], which do not show in Table 1.

Table 1: Performance comparison with reported works

		IL (dB)	Isolation (dB)	Circuit Area (λ_g^2)
[4]	1 st	2.56, 1.45	>12	0.21×0.21
	2 nd	2.39, 1.56	>12	0.14×0.16
[5]	1 st	2, 1.4	>11	0.31×0.38
	2 nd	2, 2	>12	0.28×0.33
[6]		0.65, 1	>30	0.39×0.39
[7]		1.1, 1.6	>20	0.31×0.31
[8]		0.6, 1.4	>11	0.46×0.42
[9]		2.5, 1.3	>18	0.43×0.69
This work		2.8, 1.1	>40	0.15×0.14

IV. CONCLUSION

A dual-mode dual-band BPF centered at 1.79/5.42 GHz with -3 dB FBW of 4.5%/22.5% and compact size of $0.147\lambda_g \times 0.145\lambda_g$ are presented in this paper. Compared with the reported dual-mode dual-band BPFs by using ring resonators or patch resonators in [4-9], the fabricated filter proposed in this paper has the merits of higher band-to-band isolation, higher passband selectivity, wider stopband, simpler physical configuration and design procedure. All these merits make it attractive in modern dual-band operation systems.

ACKNOWLEDGMENT

This work was supported by the Fundamental Research Funds for Central Universities under Grant 3102014JCQ01058, and the National Natural Science Foundation of China under Grant 61401358.

REFERENCES

[1] M. Hayati, A. Khajavi, and H. Abdi, "A miniaturized microstrip dual-band bandpass filter using folded UIR for multimode WLANs," *Applied Computational Electromagnetics Society (ACES) Journal*, vol. 28, no. 1, pp. 35-40, January 2013.

[2] X. Li and J. Zeng, "A novel dual-band microstrip bandpass filter design and harmonic suppression," *Applied Computational Electromagnetics Society (ACES) Journal*, vol. 28, no. 4, pp. 348-352, April 2013.

[3] Y. Ma, W. Che, W. Feng, and J. Chen, "High selectivity dual-band bandpass filter with flexible passband frequencies and bandwidths," *Applied Computational Electromagnetics Society (ACES) Journal*, vol. 28, no. 5, pp. 419-426, May 2013.

[4] Y. C. Chiou, C. Y. Wu, and J. T. Kuo, "New miniaturized dual-mode dual-band ring resonator bandpass filter with microwave C-sections," *IEEE Microw. Wireless Compon. Lett.*, vol. 20, no. 2, pp. 67-69, 2009.

[5] S. Luo, L. Zhu, and S. Sun, "A dual-band ring resonator bandpass filter based on two pairs of degenerate modes," *IEEE Trans. Microw. Theory Tech.*, vol. 58, no. 12, pp. 3427-3432, 2010.

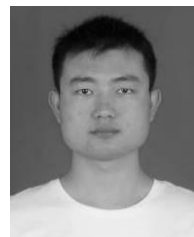
[6] S. Sun, "A dual-band bandpass filter using a single dual-mode ring resonator," *IEEE Microw. Wireless Compon. Lett.*, vol. 21, no. 6, pp. 298-300, 2011.

[7] Y. Sung, "Dual-mode dual-band filter with band notch structures," *IEEE Microw. Wireless Compon. Lett.*, vol. 20, no. 2, pp. 73-75, 2010.

[8] Y. C. Li, H. Wong, and Q. Xue, "Dual-mode dual-band filter based on a stub-loaded patch resonator," *IEEE Microw. Wireless Compon. Lett.*, vol. 21, no. 10, pp. 525-527, 2011.

[9] R. Zhang, L. Zhu, and S. Luo, "Dual-mode dual-band bandpass filter using a single slotted circular patch resonator," *IEEE Microw. Wireless Compon. Lett.*, vol. 22, no. 5, pp. 233-235, 2012.

[10] X. C. Zhang, Z. Y. Yu, and J. Xu, "Design of microstrip dual-mode filters based on source-loaded coupling," *IEEE Microw. Wireless Compon. Lett.*, vol. 18, no. 10, pp. 677-679, 2008.



Jin Xu was born in AnHui, China, in 1987. He received his B. Eng. degree in Information Countermeasure Technology and his Ph.D. degree in Information and Communication Engineering from Nanjing University of Science and Technology (NUST), Nanjing, China, in 2009 and 2014, respectively. He is currently an Associate Professor with the School of Electronics and Information, Northwestern Polytechnical University, Xi'an, China. His research interests include UWB technology, MCM technology, microwave passive/active components, microwave and millimeter-wave MMICs developed on SiGe, phased array radar and wireless communication system.

From February 2011 to September 2011, he was an attached Ph.D. student at the Institute of Microelectronics, Singapore. From October 2011 to September 2012, he joined MicroArray Technologies

Corporation Limited, Chengdu, P.R. China, where he was an IC R&D Engineer. Since 2011, he has served as a Reviewer for some journals including IEEE Microwave Wireless Component Letters, International Journal of Electronics, PIER and JEMWA.